

Chemical Science

Accepted Manuscript



This article can be cited before page numbers have been issued, to do this please use: J. R. Engstrom, A. J. Savyasachi, M. Parhizkar, A. Sutti, C. S. Hawes, J. White, T. Gunnlaugsson and F. M. Pfeffer, *Chem. Sci.*, 2018, DOI: 10.1039/C8SC01798K.



This is an Accepted Manuscript, which has been through the Royal Society of Chemistry peer review process and has been accepted for publication.

Accepted Manuscripts are published online shortly after acceptance, before technical editing, formatting and proof reading. Using this free service, authors can make their results available to the community, in citable form, before we publish the edited article. We will replace this Accepted Manuscript with the edited and formatted Advance Article as soon as it is available.

You can find more information about Accepted Manuscripts in the [author guidelines](#).

Please note that technical editing may introduce minor changes to the text and/or graphics, which may alter content. The journal's standard [Terms & Conditions](#) and the ethical guidelines, outlined in our [author and reviewer resource centre](#), still apply. In no event shall the Royal Society of Chemistry be held responsible for any errors or omissions in this Accepted Manuscript or any consequences arising from the use of any information it contains.

Norbornene chaotropic salts as low molecular mass ionic organogelators (LMIOGs)

Received 00th January 20xx,
Accepted 00th January 20xx

DOI: 10.1039/x0xx00000x

www.rsc.org/

Jordan R. Engstrom^a, Aramballi J. Savyasachi^b, Marzieh Parhizkar^c, Alessandra Sutti^c, Chris S. Hawes^d, Jonathon M. White^e, Thorfinnur Gunnlaugsson^{b*} and Frederick M. Pfeffer^{a*}

Phenylalanine functionalised norbornene (**9:Na**) functions as a potent, low molecular-mass ($M_w = 333$ Da) ionic organogelator with a minimum gelating concentration of 0.5 wt% in THF, *i*-PrOH, 1,4-dioxane and *n*-BuOH. Fibrous crystals form in the gel and X-ray crystallography identified a cation mediated helical assembly process controlled by the chirality of the phenylalanine. In addition to excellent gelating properties **9:Na** readily forms aqueous biphasic and triphasic systems.

Introduction

The development of efficient organogelating agents remains an important pursuit as the corresponding organogels have found use in sensing,^{1–3} cosmetic,^{4, 5} water purification^{6, 7} and drug delivery applications.^{8–12} Low molecular mass organogelators (LMOGs) are of particular interest as these can self-assemble using non-covalent interactions^{9, 13–16} to give rise to novel soft materials with a range of entangled and solvent dependent morphologies.^{13, 17, 18} Recently we have developed various examples of LMOGs from simple organic ligands that can, through self-association, or via coordination to either d- or f-metal ions, give rise to functional self-assembled gels.^{19–25} In parallel, our ongoing interest in applications of functionalised norbornanes and related norbornylogous systems,^{26–33} led us to synthesise simple norbornanes modified with amino-acids and here we report the development of such functionalised norbornenes as new low molecular mass *ionic* organogelators (LMIOGs) ($M_w < 350$ Da).

Ionic compounds capable of gelating organic solvents are rare and the examples that do exist are based on steroidal frameworks or they possess long alkyl chains that give rise to M_w ranging from ≈ 350 up to 1000 Da (e.g. **1–4** Figure 1).^{9, 13, 17, 34–40} Reports of compact LMIOGs, in which large hydrophobic groups have not been deliberately incorporated are extremely rare (e.g. **5** and **6**, Figure 1).^{40, 41}

Herein, we present phenylalanine norbornene **9**, a highly attractive building block for use in supramolecular self-assembly and as a LMIOG. We demonstrate, that both the (*R*) and (*S*) enantiomers participate in a chirality controlled, helical assembly process that has been characterised using X-ray crystallographic analysis, and that as a LMIOG, these form gels with fast healable rheological properties. The corresponding

xerogels consist of hollow tubular microcrystalline structures as identified using scanning electron microscopy (SEM).

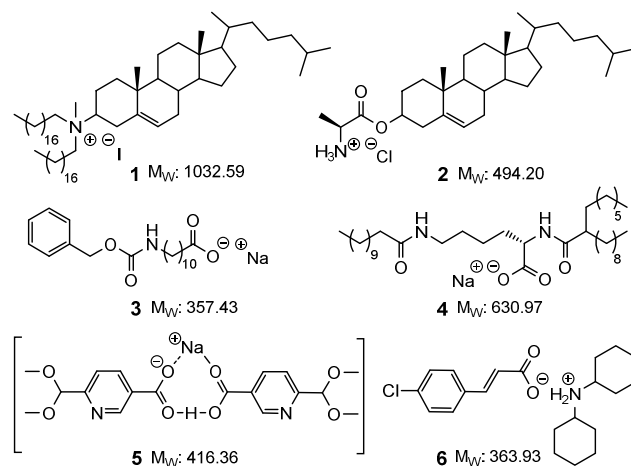


Figure 1. Examples of low molecular mass ionic organogelators. Compounds **1–4** with (and compounds **5** and **6** without) large hydrophobic groups.

Results and Discussion

During the synthesis of (*S*)-phenylalanine-functionalised norbornene (**5**)-**9** (Scheme 1) from readily available precursors a triphasic system formed upon workup using aqueous Na_2CO_3 . While there are a number of literature reports describing compound **9**, no mention of this very interesting phenomenon has been noted.^{42–46} The triphasic system (Scheme 1) was characterised as EtOAc (top layer), the added Na_2CO_3 (bottom) and the sodium salt of **9** (**9:Na**, middle).

The corresponding aqueous biphasic system could be initiated by simply mixing a concentrated (≥ 1.8 M) aqueous solution of **9:Na** with sat. Na_2CO_3 (See ESI Fig. S1.4). Aqueous biphasic systems have demonstrated utility in delicate separations such as those involving aliphatic carboxylic acids.^{47–50} The biphasic systems also formed when sat. K_2CO_3 , 5 M NaOH and 5 M KOH solutions were used. As these bases are known kosmotropic salts, the norbornene sodium salt **9:Na**, was suspected of being strongly chaotropic and the two phase system was a result of high concentrations of a kosmotrope and chaotrope.^{50–52} To confirm this theory ammonium sulphate (a kosmotropic salt) was added to a concentrated aqueous solution of **9:Na** and the rapid formation of a biphasic system validated these suspicions.

^a School of Life and Environmental Sciences, Deakin University, Waurn Ponds, Vic, 3216, (Australia). email: fred.pfeffer@deakin.edu.au

^b School of Chemistry and Trinity Biomedical Sciences Institute (TBSI), Trinity College Dublin, the University of Dublin, Dublin 2 (Ireland). email: gunnlaut@tcd.ie

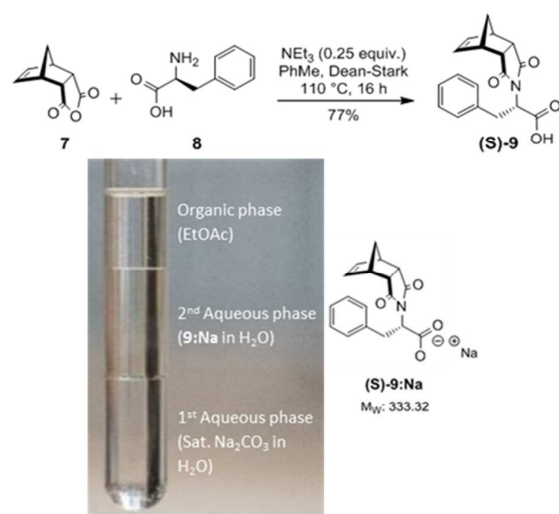
^c Institute for Frontier Materials, Deakin University, Waurn Ponds, Vic, 3216, (Australia).

^d School of Chemical and Physical Sciences, Keele University, Staffordshire, ST5 5BG (UK).

^e Bio21 Institute, School of Chemistry, University of Melbourne, Parkville, 3010 (Australia).

Electronic Supplementary Information (ESI) available: synthesis, NMR diffusion, gelation, SEM images, DSC thermograms, rheological data and crystallographic data in CIF format. See DOI: 10.1039/x0xx00000x





Scheme 1. Top: Synthesis of phenylalanine-functionalised norbornene (**S**)-**9**. Bottom: triphasic system formed by mixing (**S**)-**9** with sat. Na₂CO₃ and EtOAc.

Further evidence of the chaotropic nature was obtained using ¹H NMR diffusion experiments that showed an *increase* in the diffusion rate as the concentration of **9:Na** was elevated (Figure 2, See ESI section S2 for details). This is likely caused by a decrease in the viscosity of the D₂O, which can in turn, be attributed to the known ability of chaotropic salts to “disrupt” the structure of water.⁵³⁻⁵⁵

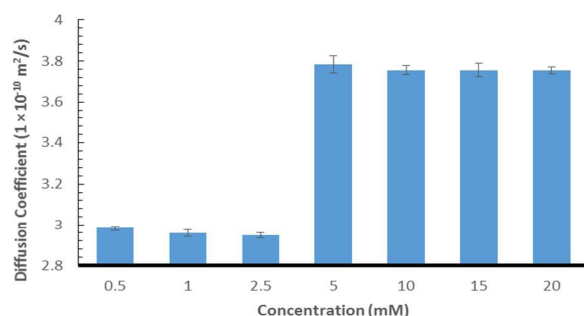


Figure 2. Diffusion coefficient of **9:Na** in water in relation to concentration

Organogelation

It was also noted that **9:Na** was exceptionally water soluble, up to 3 g/mL with heating. Upon cooling, this highly concentrated solution formed a hydrogel (rather than a precipitate) with gel formation likely caused by assembly of a supramolecular polymer.^{56, 57} Other concentrated solutions (2–2.5 g/mL), did not form gels; instead resulting in the formation of highly viscous solutions, as shown in Figure 3, again indicating that a larger assembly was likely to be forming under these experimental conditions.

During the characterisation of the biphasic and triphasic systems, it was serendipitously discovered that addition of small amounts (10 μL) of aqueous **9:Na** (≥ 3 M) to a variety of organic solvents (1.0 mL) resulted in the rapid formation of clear gels. As such, a range of salts of **9** were prepared,

including Ca²⁺, K⁺, Na⁺, Li⁺ as well as the tetramethylammonium (TMA), tetraethylammonium (TEA) and tetrabutylammonium (TBA), and their gelating properties were investigated in various protic and aprotic solvents including EtOH, *i*-PrOH, *n*-BuOH, 1,4-Dioxane, THF, CHCl₃ and PhMe.



Figure 3. Concentrated aqueous solutions of **9:Na**; from left to right: 1, 2, 2.5 and 3 g/mL.

This investigation showed that the calcium salt failed to elicit gel formation in any of the solvents trialled, demonstrating that this salt was not functioning as LMIOG. However, when small amounts (4 mg) of the potassium salt **9:K** were added to a range of these solvents (200 μL) and heated, on cooling the formation of soft-materials with strong gel-like properties (withstanding the classic inversion test) was observed in both *i*-PrOH and *n*-BuOH, while a weak gel was formed in PhMe (Table 1). These results clearly demonstrate the ability of **9:K** to function as LMIOG in a broad range of solvents.

Table 1. Gelation of organic solvents (minimum gelation concentration)

Solvent	9:K ^a	9:Na ^a
Methanol	D	D
Ethanol	D	G ^a (2 wt%) ^b
Isopropanol	TG (2 wt%) ^b	G ^a (0.5 wt%) ^{b,c}
<i>n</i> -Butanol	TG (2 wt%) ^b	G ^a (0.5 wt%) ^{b,c}
Dioxane	A	G ^b (0.5 wt%) ^c
Tetrahydrofuran	I	G ^b (0.5 wt%) ^c
Diethyl Ether	I	I
Acetone	A	PG
Ethyl Acetate	A	PG
Dimethylformamide	D	D
Dimethyl sulfoxide	D	D
Acetonitrile	I	A
Chloroform	A	WG (1 wt%) ^b
Dichloromethane	A	S
Toluene	S	A
Pet. Spirits (40-60 °C)	I	I
Heptane	I	I

a) Gelator added as a powder (2 mg/mL⁻¹) b) Minimum gelator concentration (MGC) established using solid **9:K** or **9:Na**—see ESI section S3 for full details c) MGC established using 3.0 M solution of **9:K** or **9:Na**—see ESI for full details. G = Clear gel, WG = Weak gel, PG = Partial gel, S = Suspension, D = Dissolved, I = Insoluble, A = Aggregate, TG = Turbid gel.

We next investigated the morphological features of the gels generated from the chaotropic salt **9:K**. Imaging, using SEM, of the xerogel formed from the **9:K** *i*-PrOH gel identified



an entangled web of fibrils with average diameter ≈ 200 nm (shown in Figure 4a, see also ESI section S4) and such morphology is typical for gelatinous materials. While the fibres identified from the gel formed in *n*-BuOH (Figure 4b) appeared more linear and needle-like, the typical entangled morphology was maintained.

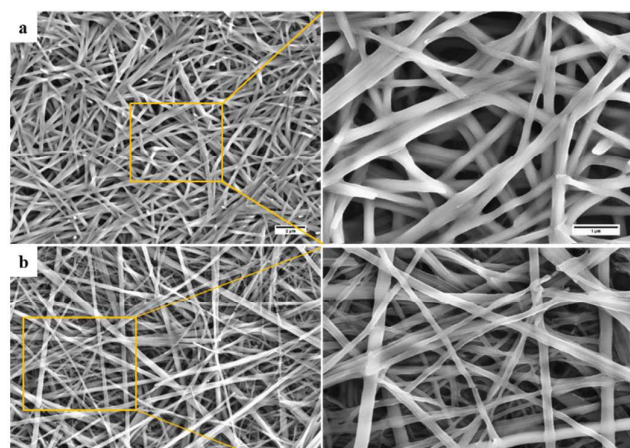


Figure 4. SEM images of 9:K thin film in (a) *i*-PrOH (2 wt%), (b) *n*-BuOH (2 wt%)

The sodium salt **9:Na** was a potent organogelator (Table 1) and using the solid material (4 mg added to 200 μ L of a solvent) robust soft-materials, that withstood inversion tests, were obtained from EtOH, *i*-PrOH, *n*-BuOH, THF and 1,4-dioxane, whereas weaker gels were observed to form in solvents such as CHCl_3 and CH_2Cl_2 .

The gelation experiments were also carried out by using a 5 μ L addition of a 3 M aqueous solution of **9:Na** (50 μ g in 50 μ L of H_2O , see ESI section S3 for full details) to the organic solvents (1 mL) followed by sonication of the resulting mixture. Formation of gels in *i*-PrOH, THF and 1,4-dioxane was again observed at low gelator concentration (0.5 wt%). The formation of gels in both THF and 1,4-dioxane occurred extremely rapidly, especially in the case of THF, which was observed to gelate immediately after addition of the **9:Na** solution without the need of using either heat or sonication to trigger the gelation process, again demonstrating that this salt could function as a potent LMIOG.

The SEM images of the xerogels formed from the EtOH and *i*-PrOH gels were largely devoid of the long fibrils observed previously, instead a fibrous matlike residue was seen (Figure 5). The lack of fibrils was believed to be due to the extremely rapid gelation process that occurred before extended fibril formation could take place.

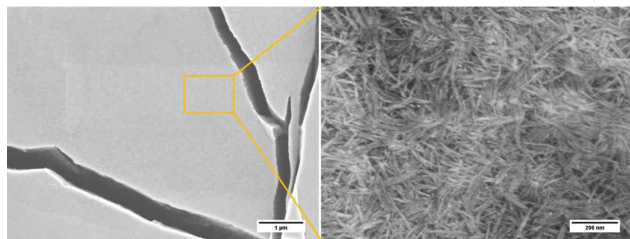


Figure 5. SEM images of xerogel obtained from 9:Na EtOH gel (2 wt%).

When the SEM imaging experiments were performed using a larger sample of the *i*-PrOH gel (20–30 μ L) hollow hexagonal columnar structures (1–3 μ m across) were observed in the resulting xerogel (Figure 6). Recently, the group of Hardie identified a similar architecture from the crystallisation of a large bowl shaped cyclotrimeratrylene (M_w 723.74) with CuBr_2 ,⁵⁸ and previous work by Li and co-workers revealed that a structurally similar compound, diphenylalanine, was also capable of assembly into hollow hexagonal crystal.⁵⁹ Hollow hexagonal crystals were also reported from the self-assembly of cyclic peptides in a liquid crystal by Dory *et al.*⁶⁰ Very recently, Pasan *et al.* reported the use of Ostwald ripening to grow ~ 300 μ m sized hollow crystals, from a planar trinuclear Cu(II)-cyamelurate complex.⁶¹ The crystals identified by Pasan possessed hollow hexagonal prismatic morphology, very similar to that identified here, demonstrating the growth of larger sized (micron) hollow tubular structures from a bulk solution.⁶¹ Nevertheless, such nanometre-scale morphology is remarkably rare and to the best of our knowledge, the work presented herein, is the first instance where such topology has been observed in a xerogel formed from LMIOGs. The hollow hexagons were reproducibly formed from *i*-PrOH at a range of gelator concentrations (0.5–2 wt%). These organogels were found to be stable over several months, and no change was observed in their morphological features when SEM images were recorded.

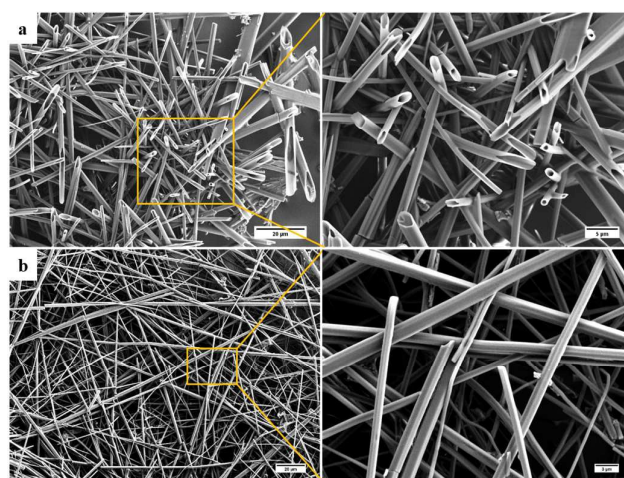


Figure 6. SEM images of 9:Na xerogel obtained from (a) *i*-PrOH (1 wt%) showing hollow hexagons and (b) *n*-BuOH (1 wt%) showing rods.

These hollow tubes were not observed in any other solvent indicating a remarkable solvent effect on the nanoscale morphology. In *n*-BuOH (Figure 6) similar intertwined rods (0.5–2 μ m) formed; yet in comparison to the hollow hexagons systems, these appeared more solid, narrower, and somewhat flexible. Gels from **9:Na** in hydrophilic solvents, especially *i*-PrOH and *n*-BuOH, were stable to the inversion test for periods of several weeks before fine needle-like crystals became evident (Figure 7) eventually leading to gel collapse. Gels in volatile hydrophobic solvents, especially CH_2Cl_2 and CHCl_3 ,



were not as stable, lasting only a few days (unless carefully sealed to prevent solvent evaporation) before crystals formed and the gel collapsed.

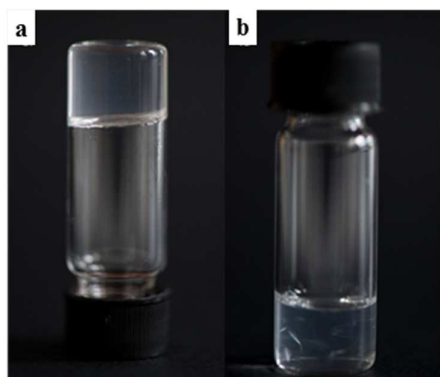


Figure 7. a) A clear gel formed using **9:Na** in *i*-PrOH (1 wt%); b) crystals of **9:Na** forming in a 1,4-dioxane gel (1 wt%) after 7 days;

In contrast to these results, for the lithium salt **9:Li**, no gels could be reliably obtained, although evidence of aggregation was observed in 1,4-dioxane solution at slightly higher concentration (2 wt%) and only if this hygroscopic salt was rigorously dried prior to the gelation tests, ruling out the use of this system as a LMIOG. When this aggregate was examined using SEM, unique hexagonal microcrystals (ca. $15 \times 3 \mu\text{m}$) were revealed (Figure 8).

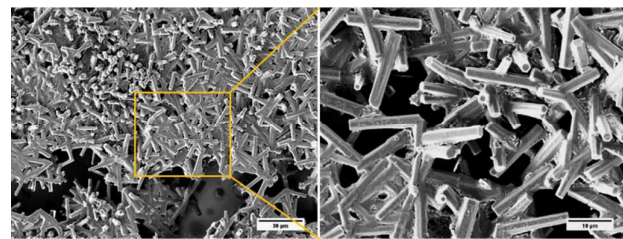


Figure 8. SEM images of **9:Li** xerogel from 1,4-dioxane (2 wt%).

The structural variation in xerogel morphology clearly indicates the role of both the counterions and the solvent. Unfortunately, the tetraalkylammonium salts of **9** proved to be very hygroscopic, and consequently, none were capable of initiating a biphasic system nor the formation of a soft-material in any solvent, instead these tetraalkylammonium salts were readily soluble in most of the organic solvents tested (see ESI section S3 for details of evaluation).

Varying the gelator structure

In addition to examining the role of the counterion in gel formation, additional structural modifications using amino acids were pursued. The tryptophan (**10**), tyrosine (**11**) and alanine (**12**) analogues of **9** (Figure 9) were all readily synthesised (See ESI section S1 for details). While the tryptophan functionalised norbornene **10** formed a triphasic system when washed with a saturated Na_2CO_3 solution, the isolated sodium salt **10:Na** failed to elicit gel formation in any

solvent trialled. Similarly, both **11:Na** and **12:Na** showed similar behaviour and were not able to function as LMIOG.

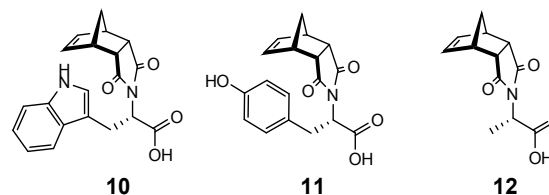


Figure 9. Tryptophan, Tyrosine and alanine functionalised norbornenes **10-12**.

To investigate the effects of chirality on the self-assembly and gelation process, (*R*)-phenylalanine (Figure 10) was also synthesised and used to generate (*R*)-**9:Na**. As expected, this enantiomer and its behaviour was identical in all aspects to the (*S*) stereoisomer including the formation of the biphasic system, confirming that this enantiomer could also function as a LMIOG. Of interest, it was noted that a racemic mixture of (*R*) and (*S*)-**9:Na** failed to form gel material in any of the solvent systems employed above, indicating that the supramolecular assembly process leading to solvent entanglement possibly also relied on the presence of a single enantiomer.^{8, 62-66}

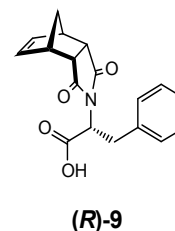


Figure 10. (*R*)-Phenylalanine functionalised norbornene (*R*)-**9**.

Rheological evaluation

Having investigated the morphological features of the various xerogels, we set out to probe the mechanical properties of the gels formed by **9:K** and **9:Na** by carrying out dynamic rheological measurements, which included frequency and strain sweep and recovery tests. Prior to these investigations, Differential Scanning Calorimetry (DSC) was performed on the gel samples and the results revealed that these gels had sharp gel-sol transition points 20-30 °C below the boiling point of the solvent (see ESI Table S5.1, section S5).

Frequency sweep experiments showed elastic response in the linear viscoelastic regime, wherein, the storage modulus (G') was consistently higher than the loss modulus (G'') across all samples, as shown for the 1% **9:Na** gel formed in *i*-PrOH in Figure 11 (see ESI section S6 for all rheological results), confirming the solid like behaviour of the gels. Both the *i*-PrOH and *n*-BuOH gels of **9:K** (2 wt%) possessed comparable rheological behaviour; a result that correlated well with the SEM observations where both gels had similar morphological features. Both the elasticity ($G' = 1.35 \times 10^4$ and 7.3×10^4 Pa for 2 wt% *i*-PrOH and *n*-BuOH gels respectively) and the stiffness ($G'/G'' = 6.2$ and 7.3 for 6.2 for *i*-PrOH and *n*-BuOH) were



similar, though the *n*-BuOH gel was found to be slightly stronger, as summarised in Table 2. The yield stress for both gels were also similar ($\sigma^* \sim 10\%$). As **9:Na** formed gels in a larger assortment of organic solvents, a broader range of rheological behaviour was observed (Table 2). Typically the **9:Na** gels were stronger than their **9:K** counterparts, however, gel strength did not show any particular relationship with the solvent used.

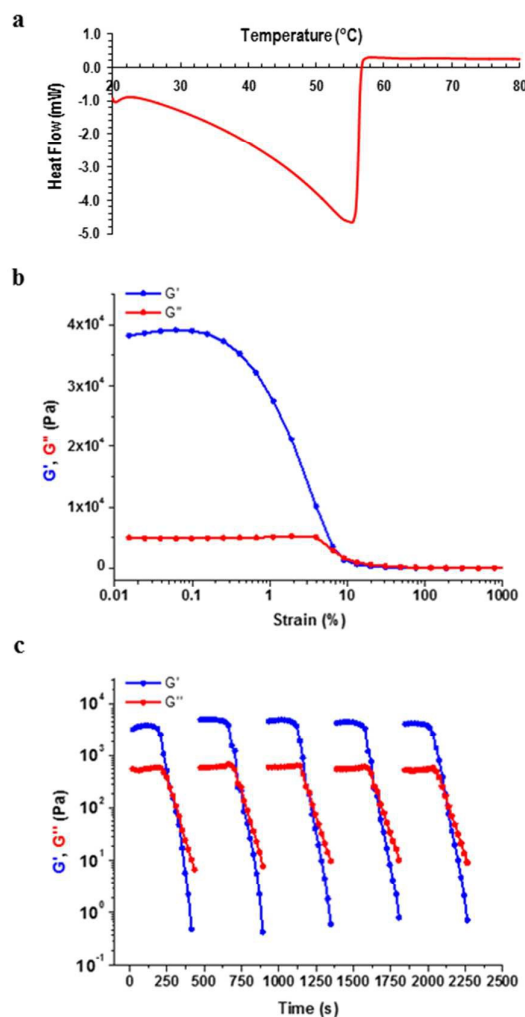


Figure 11. Characterisation of the 1 wt% gel formed by **9:Na** in *i*-PrOH (A) DSC (B) Rheological strain sweep and (C) Rheological recovery test.

As mentioned above, the stiffness (G'/G'') and yield strain (σ^*) values correlated well to the morphological features of the xerogels that were observed using SEM (Figure 12), and such a relationship suggests that the fibrils may be organised in similar arrangements in the corresponding gels. The lower G' value for EtOH gel is likely to be due to the formation of smaller fibrils that lack the extended entanglement. In contrast, for the stronger **9:Na** *i*-PrOH gel, the larger micrometre sized (1–3 μm diameter) hollow columnar structures in its gel matrix (*vide supra*) are likely contributors to the greater overall gel strength.

Table 2. Dynamic rheology results for **9:K** and **9:Na** gels.^a

Gelator (wt%)/solvent	G' (Pa)	Stiffness (G'/G'')	σ^* (Pa)
9:K (2 wt%)/ <i>i</i> -PrOH	1.4×10^4	6.2	9.4%
9:K (2 wt%)/ <i>n</i> -BuOH	7.3×10^4	7.3	9.8%
9:Na (2 wt%)/EtOH	6.9×10^3	7.7	5.6%
9:Na (1 wt%)/ <i>i</i> -PrOH	3.8×10^4	7.6	7.5%
9:Na (2 wt%)/ <i>i</i> -PrOH	1.1×10^5	10.1	15%
9:Na (2 wt%)/ <i>n</i> -BuOH	2×10^4	3.8	8.6%
9:Na (2 wt%)/1,4-Dioxane	1.2×10^5	4.8	4.4%
9:Na (2 wt%)/CHCl ₃	1.6×10^5	4.6	4.5%
9:Na (2 wt%)/THF	1.7×10^5	3.2	0.4%

^a G' , G'' and σ^* values were obtained from strain sweep experiments performed at fixed frequency of 1 Hz.

Both **9:K** and **9:Na** gels showed remarkable recovery properties; for the **9:Na** gel in *i*-PrOH (1 wt%) (Figure 11C) applying a strain amplitude of 100% resulted in liquid like behaviour ($G'' > G'$). However, the original gel state ($G' > G''$) instantly recovered when the strain was reduced to 0.1%. Recovery was observed over multiple cycles of measurements and all **9:K** and **9:Na** gels showed similar recovery behaviour within the 30–40 second interval between alternating strain regimes (see ESI for full details). These results demonstrate the thixotropic properties of the gels generated from these LMIOGs and suggest their potential as self-healing materials.

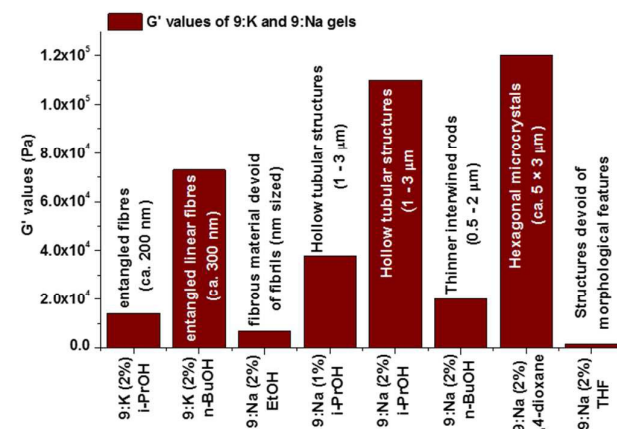


Figure 12. The variation of G' values of **9:K** and **9:Na** gels and the morphology of the corresponding gels.

Supramolecular assembly and crystal structure

In addition to carrying out the investigation into the ability of these LMIOGs to form soft-materials, we were also able to form crystalline material from these gels. Long needle like crystals of (**S**)-**9:Na** that were suitable for X-ray analysis were obtained upon crystallisation from its *i*-PrOH gel (Figure 7) and revealed that individual units of the norbornene adopt an amphiphilic structure in the solid state, with the norbornene framework and the phenylalanine aromatic positioned in close



proximity (potentially through C(sp²)-H π interactions)⁶⁷⁻⁶⁹ and the carboxylate residue oriented away from the hydrophobic portions (Figure 13). This conformational arrangement was also evident in solution as the ¹H NMR spectrum of **9** (see ESI figure S1.1) revealed one of the norbornene C(sp²)-H resonances significantly upfield (δ = 5.33 ppm) from the other (δ = 5.62 ppm). Such a shift is indicative of anisotropic shielding due to the proximity of the aromatic ring current from the closely positioned phenylalanine residue.^{70, 71}

Using identical conditions, the structure of the (*R*)-**9:Na** enantiomer was also characterised and, as predicted, revealed the structural mirror image (Figure 13). The racemate showed no evidence of gelation or crystal formation.

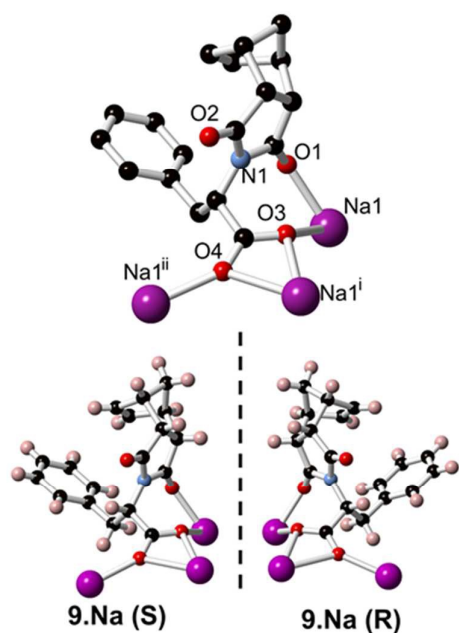


Figure 13. Crystal structure of both (*S*) and (*R*)-**9:Na**

Further investigation into the long range interactions in the crystal structures revealed that the individual monomers assembled into hollow, helical columns (shown in Figure 14a) with the helical assembly being mediated by the Na⁺ ions that adopt an irregular six-coordinate geometry. Four of these coordination sites are occupied by carboxylate groups with the final two sites being occupied by a water ligand and the imide oxygen *syn* to the chiral centre. It is this imide coordination that controls the direction of the helix, resulting in a right-handed conformation for (*S*)-**9:Na** and left-handed for (*R*)-**9:Na** (Figure 14b).⁷² The helix has a pitch of 19.8 Å and a diameter of 19.6 Å, with 6 monomer residues per complete turn. Each additional monomer represents a 60° turn in the helix and a 3.2 Å translation along the helical axis.

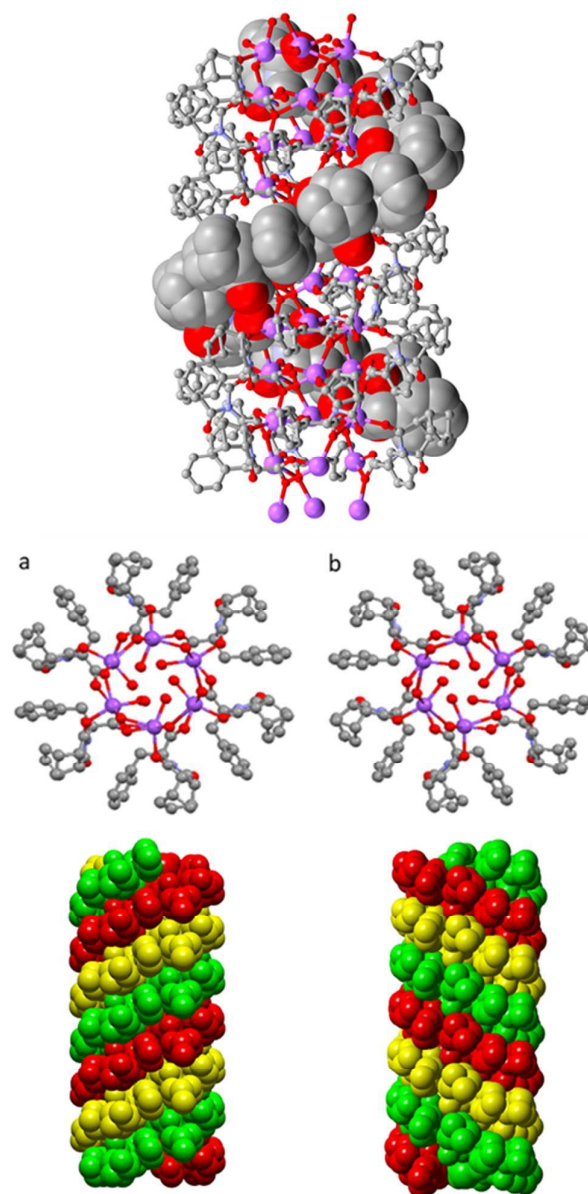


Figure 14. Helical columns formed by the self-assembly of (a) (*S*)-**9:Na** and (b) (*R*)-**9:Na** in *i*-PrOH observed in the crystal structure.

Adjacent stacks in the structure of (*S*)-**9:Na** associate in a hexagonal rod packing fashion with hydrophobic interactions between the outwards facing organic periphery. No significant voids were observed in the interstitial spaces, indicating efficient packing of the homochiral helices. This observation offers some justification as to the need for enantiomeric purity as given the significant undulation in the external surface of the columns and the numerous intermolecular contacts (clearly visible using Hirshfeld surface mappings, see ESI, Figure S7.3), co-crystallisation of helices with alternate handedness would be expected to lead to a significant decrease in packing efficiency.



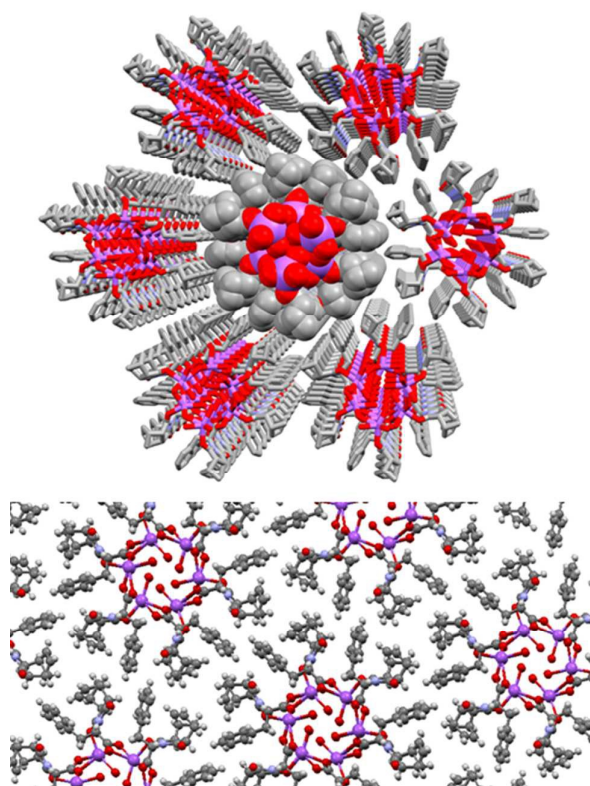


Figure 15. The full crystal network of (S)-9:Na showing two views of the repeating columnar helical assemblies and their interactions.

As a model for assembly, the largely hydrophobic structure of **9** protects the hydrophilic carboxylate by assembling such that the carboxylate is shielded from the organic solvent. As the amphiphile is chiral, a helical assembly occurs in which all carboxylates are oriented to the interior of the helix ensuring that they are not solvent exposed.

A crystal structure of the non-gelating salt (S)-9:TEA was also obtained and revealed the formation of thin ribbons (Figure 16). In this example the counterions did not take part in the formation of the ribbons, instead only being loosely associated with the carboxylate moieties, demonstrating the importance of the small sodium cation in the helical assembly process for **9:Na**. Of additional interest, the X-ray structure of (S)-9:TEA revealed alternating cyclic tetramers of water and loops involving both water molecules and the carboxylate receptor as demonstrated in Figure 16.⁷³⁻⁷⁷

Conclusions

The results presented here show that compound **9:Na** is a highly capable small molecule that can function as a low molecular weight ionic organogelator (LMIOG). This ionic compound can readily form biphasic and triphasic systems and, in the solid state assembles to form chiral helical columns. In addition **9:Na** acts as an efficient ionic organogelator in a variety of organic solvents at concentrations as low as 0.5 wt%. The rheological measurements of the gels formed also

demonstrate rapid recovery and that these organogels have potential as self-healing materials. Such interesting behaviour reinforces the importance of supramolecular assembly as a means to control macroscopic behaviour and also the requirement for careful characterisation to aid in the understanding of fundamental molecular level interactions. We are in the process of developing other LMIOGs and investigating their properties and applications.

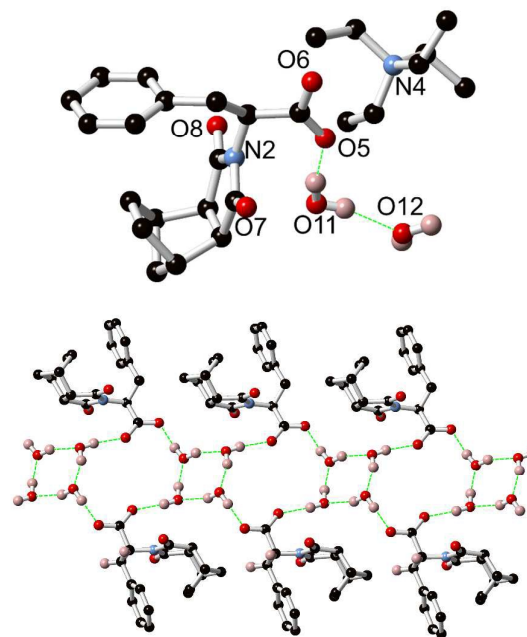


Figure 16. Top: Crystal structure of **9:TEA** showing the loose association of the TEA counterion. Non-bonding hydrogens have been omitted for clarity. Bottom: Crystal structure of **9:TEA** highlighting both the ribbon structure and the role of water in the assembly. The TEA counterions and non-bonding hydrogens have been omitted for clarity.

Acknowledgements

FP and JE thank the Deakin Centre for Chemistry and Biotechnology and also the Australian Research Council (DP140100227) for financial support. AS and MP thank the Australian Research Council Future Fibre Industry Transformation Research Hub (IH140100018) for financial support. TG thanks Science Foundation Ireland (SFI) for financial support (SFI PI Award 13/IA/1865). Donna Edwards is acknowledged for the photos of the triphasic system and the gels (Scheme 1, Figure 3 and Figure 7).

References

1. B. K. An, D. S. Lee, J. S. Lee, Y. S. Park, H. S. Song and S. Y. Park, *J Am Chem Soc*, 2004, **126**, 10232-10233.
2. P. C. Xue, Q. X. Xu, P. Gong, C. Qian, A. M. Ren, Y. Zhang and R. Lu, *Chemical Communications*, 2013, **49**, 5838-5840.



ARTICLE

Journal Name

3. S. Bhattacharya, S. Sarkar and R. Shunmugam, *Journal of Materials Chemistry A*, 2013, **1**, 8398-8405.
4. M. E. Morales, V. Gallardo, B. Clares, M. B. Garcia and M. A. Ruiz, *Journal of Cosmetic Science*, 2009, **60**, 627-636.
5. P. L. Luisi, R. Scartazzini, G. Haering and P. Schurtenberger, *Colloid Polym Sci*, 1990, **268**, 356-374.
6. S. Debnath, A. Shome, S. Dutta and P. K. Das, *Chemistry-A European Journal*, 2008, **14**, 6870-6881.
7. E. J. Cho, I. Y. Jeong, S. J. Lee, W. S. Han, J. K. Kang and J. H. Jung, *Tetrahedron Letters*, 2008, **49**, 1076-1079.
8. A. Vintiloiu and J.-C. Leroux, *J. Controlled Release*, 2008, **125**, 179-192.
9. K. J. Skilling, F. Citossi, T. D. Bradshaw, M. Ashford, B. Kellam and M. Marlow, *Soft Matter*, 2014, **10**, 237-256.
10. N. M. Sangeetha and U. Maitra, *Chem. Soc. Rev.*, 2005, **34**, 821-836.
11. A. Ajayaghosh and V. K. Praveen, *Acc. Chem. Res.*, 2007, **40**, 644-656.
12. J. A. Foster, K. K. Damodaran, A. Maurin, G. M. Day, H. P. Thompson, G. J. Cameron, J. C. Bernal and J. W. Steed, *Chemical science*, 2017, **8**, 78-84.
13. P. Terech and R. G. Weiss, *Chem. Rev.*, 1997, **97**, 3133-3160.
14. R. G. Weiss, *J. Am. Chem. Soc.*, 2014, **136**, 7519-7530.
15. L. Meazza, J. A. Foster, K. Fucke, P. Metrangolo, G. Resnati and J. W. Steed, *Nature chemistry*, 2013, **5**, 42.
16. A. J. Savyasachi, O. Kotova, S. Shanmugaraju, S. J. Bradberry, G. M. Ó'Máille and T. Gunnlaugsson, *Chem*, 2017, **3**, 764-811.
17. D. J. Abdallah and R. G. Weiss, *Adv. Mater.*, 2000, **12**, 1237-1247.
18. R. Daly, O. Kotova, M. Boese, T. Gunnlaugsson and J. J. Boland, *ACS nano*, 2013, **7**, 4838-4845.
19. M. Martínez-Calvo, O. Kotova, M. E. Möbius, A. P. Bell, T. McCabe, J. J. Boland and T. Gunnlaugsson, *J. Am. Chem. Soc.*, 2015, **137**, 1983-1992.
20. J. I. Lovitt, C. S. Hawes, A. D. Lynes, B. Haffner, M. E. Möbius and T. Gunnlaugsson, *Inorganic Chemistry Frontiers*, 2017, **4**, 296-308.
21. S. J. Bradberry, A. J. Savyasachi, R. D. Peacock and T. Gunnlaugsson, *Faraday Discuss.*, 2015, **185**, 413-431.
22. C. S. Hawes, A. D. Lynes, K. Byrne, W. Schmitt, G. Ryan, M. E. Möbius and T. Gunnlaugsson, *Chem. Commun.*, 2017, **53**, 5989-5992.
23. C. S. Hawes, Y. Nolvachai, C. Kulsing, G. P. Knowles, A. L. Chaffee, P. J. Marriott, S. R. Batten and D. R. Turner, *Chem. Commun.*, 2014, **50**, 3735-3737.
24. E. P. McCarney, J. P. Byrne, B. Twamley, M. Martínez-Calvo, G. Ryan, M. E. Möbius and T. Gunnlaugsson, *Chem. Commun.*, 2015, **51**, 14123-14126.
25. O. Kotova, R. Daly, C. I. M. dos Santos, P. E. Kruger, J. J. Boland and T. Gunnlaugsson, *Inorg. Chem.*, 2015, **54**, 7735-7741.
26. M. D. Johnstone, E. K. Schwarze, G. H. Clever and F. M. Pfeffer, *Chemistry-A European Journal*, 2015.
27. M. D. Johnstone, M. Frank, G. H. Clever and F. M. Pfeffer, *Eur. J. Org. Chem.*, 2013, **2013**, 5848-5853.
28. R. N. Robson and F. M. Pfeffer, *Chem. Commun.*, 2016, **52**, 8719-8721.
29. A. J. Lowe, B. M. Long and F. M. Pfeffer, *Chem. Commun.*, 2013, **49**, 3376-3388.
30. F. M. Pfeffer, T. Gunnlaugsson, P. Jensen and P. E. Kruger, *Org. Lett.*, 2005, **7**, 5357-5360.
31. F. M. Pfeffer, P. E. Kruger and T. Gunnlaugsson, *Org. Biomol. Chem.*, 2007, **5**, 1894-1902.
32. S. M. Hickey, T. D. Ashton, S. K. Khosa, R. N. Robson, J. M. White, J. Li, R. L. Nation, Y. Y. Heidi, A. G. Elliott and M. S. Butler, *Organic & biomolecular chemistry*, 2015, **13**, 6225-6241.
33. S. M. Hickey, T. D. Ashton, J. M. White, J. Li, R. L. Nation, Y. Y. Heidi, A. G. Elliott, M. S. Butler, J. X. Huang and M. A. Cooper, *RSC advances*, 2015, **5**, 28582-28596.
34. X. Huang and R. G. Weiss, *Tetrahedron*, 2007, **63**, 7375-7385.
35. M. George, G. P. Funkhouser and R. G. Weiss, *Langmuir*, 2008, **24**, 3537-3544.
36. G. Mieden-Gundert, L. Klein, M. Fischer, F. Vögtle, K. Heuzé, J. L. Pozzo, M. Vallier and F. Fages, *Angewandte Chemie International Edition*, 2001, **40**, 3164-3166.
37. M. Suzuki, M. Yumoto, M. Kimura, H. Shirai and K. Hanabusa, *Helvetica chimica acta*, 2004, **87**, 1-10.
38. Y. Li, K. Liu, J. Liu, J. Peng, X. Feng and Y. Fang, *Langmuir*, 2006, **22**, 7016-7020.
39. D. J. Abdallah and R. G. Weiss, *Journal of the Brazilian Chemical Society*, 2000, **11**, 209-218.
40. D. Bardelang, F. Camerel, A. C. Hotze, B. Kariuki, B. Paik, M. Schmutz, R. Ziessel and M. J. Hannon, *Chemistry*, 2007, **13**, 9277-9285.
41. D. R. Trivedi, A. Ballabh and P. Dastidar, *Chemistry of Materials*, 2003, **15**, 3971-3973.
42. S. K. Baloch, L. Ma, X.-L. Wang, J. Shi, Y. Zhu, F.-Y. Wu, Y.-J. Pang, G.-H. Lu, J.-L. Qi and X.-M. Wang, *RSC Advances*, 2015, **5**, 31759-31767.
43. A. Bodtke and H.-H. Otto, *Die Pharmazie-An International Journal of Pharmaceutical Sciences*, 2005, **60**, 803-813.
44. H. Zhou, E.-M. Schön, M. Wang, M. J. Glassman, J. Liu, M. Zhong, D. Díaz Díaz, B. D. Olsen and J. A. Johnson, *J. Am. Chem. Soc.*, 2014, **136**, 9464-9470.
45. C. P. Hackenberger, I. Schiffers, J. Runsink and C. Bolm, *The Journal of organic chemistry*, 2004, **69**, 739-743.
46. M. R. Buchmeiser, F. Sinner, M. Mupa and K. Wurst, *Macromolecules*, 2000, **33**, 32-39.
47. J. Rydberg, *Solvent extraction principles and practice, revised and expanded*, CRC Press, 2004.
48. M. Iqbal, Y. Tao, S. Xie, Y. Zhu, D. Chen, X. Wang, L. Huang, D. Peng, A. Sattar and M. A. B. Shabbir, *Biological procedures online*, 2016, **18**, 18.
49. Y. Pei, J. Wang, K. Wu, X. Xuan and X. Lu, *Sep. Purif. Technol.*, 2009, **64**, 288-295.
50. M. T. Zafarani-Moattar and S. Hamzehzadeh, *Journal of Chemical & Engineering Data*, 2010, **55**, 1598-1610.
51. N. J. Bridges, K. E. Gutowski and R. D. Rogers, *Green Chemistry*, 2007, **9**, 177-183.
52. N. J. Bridges and R. D. Rogers, *Sep. Sci. Technol.*, 2008, **43**, 1083-1090.
53. B. Hribar, N. T. Southall, V. Vlachy and K. A. Dill, *J. Am. Chem. Soc.*, 2002, **124**, 12302-12311.
54. A. S. Parmar and M. Muschol, *Biophys. J.*, 2009, **97**, 590-598.
55. R. Zangi, *The Journal of Physical Chemistry B*, 2009, **114**, 643-650.



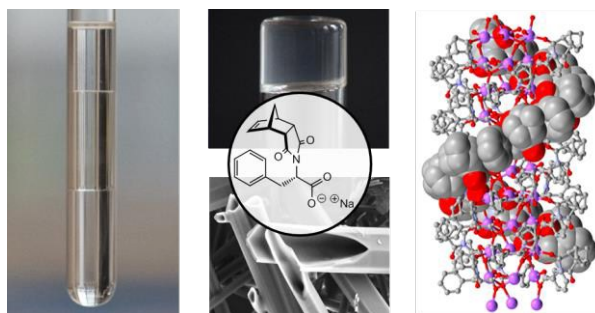
56. L. N. Neumann, M. B. Baker, C. M. Leenders, I. K. Voets, R. P. Lafleur, A. R. Palmans and E. W. Meijer, *Organic & biomolecular chemistry*, 2015, **13**, 7711-7719.
57. B. Isare, S. Pensec, M. Raynal and L. Bouteiller, *Comptes Rendus Chimie*, 2016, **19**, 148-156.
58. F. L. Thorp-Greenwood, A. N. Kulak and M. J. Hardie, *Nature chemistry*, 2015, **7**, 526-531.
59. X. Yan, J. Li and H. Möhwald, *Adv. Mater.*, 2011, **23**, 2796-2801.
60. S. Leclair, P. Baillargeon, R. Skouta, D. Gauthier, Y. Zhao and Y. L. Dory, *Angew. Chem. Int. Ed.*, 2004, **43**, 349-353.
61. C. Martínez-Benito, A. Bauzá, A. B. Lago, C. Ruiz-Pérez, C. A. Jiménez, M. E. Torres, A. Frontera and J. Pasán, *Cryst. Growth Des.*, 2018, DOI: 10.1021/acs.cgd.8b00305.
62. A. R. Hirst, D. K. Smith, M. C. Feiters and H. P. Geurts, *Chemistry-A European Journal*, 2004, **10**, 5901-5910.
63. K. Hanabusa, Y. Maesaka, M. Kimura and H. Shirai, *Tetrahedron Lett.*, 1999, **40**, 2385-2388.
64. K. Hanabusa, K. Okui, K. Karaki, M. Kimura and H. Shirai, *J. Colloid Interface Sci.*, 1997, **195**, 86-93.
65. J. H. Fuhrhop, P. Schnieder, J. Rosenberg and E. Boekema, *J. Am. Chem. Soc.*, 1987, **109**, 3387-3390.
66. J. H. Fuhrhop and W. Helfrich, *Chem. Rev.*, 1993, **93**, 1565-1582.
67. Z. Zhang, Y. Luo, J. Chen, S. Dong, Y. Yu, Z. Ma and F. Huang, *Angew. Chem.*, 2011, **123**, 1433-1437.
68. J. F. Malone, C. M. Murray, M. H. Charlton, R. Docherty and A. J. Lavery, *J. Chem. Soc., Faraday Trans.*, 1997, **93**, 3429-3436.
69. M. Nishio, Y. Umezawa, M. Hirota and Y. Takeuchi, *Tetrahedron*, 1995, **51**, 8665-8701.
70. R. M. Silverstein and G. C. Bassler, *J. Chem. Educ.*, 1962, **39**, 546.
71. C. S. Wannere and P. v. R. Schleyer, *Org. Lett.*, 2003, **5**, 605-608.
72. Z. Shen, T. Wang and M. Liu, *Angew. Chem. Int. Ed.*, 2014, **53**, 13424-13428.
73. R. Ludwig, *Angew. Chem. Int. Ed.*, 2001, **40**, 1808-1827.
74. M. Mascal, L. Infantes and J. Chisholm, *Angew. Chem. Int. Ed.*, 2006, **45**, 32-36.
75. O. Fabelo, J. Pasán, L. Cañadillas-Delgado, F. S. Delgado, A. Labrador, F. Lloret, M. Julve and C. Ruiz-Pérez, *CrystEngComm*, 2008, **10**, 1743-1746.
76. L.-S. Long, Y.-R. Wu, R.-B. Huang and L.-S. Zheng, *Inorg. Chem.*, 2004, **43**, 3798-3800.
77. S. Supriya, S. Manikumari, P. Raghavaiah and S. K. Das, *New J. Chem.*, 2003, **27**, 218-220.



Norbornene chaotropic salts as low molecular mass ionic organogelators (LMIOGs)

Jordan R. Engstrom^a, Aramballi J. Savyasachi^b, Marzieh Parhizkar^c, Alessandra Sutti^c, Chris S. Hawes^d, Jonathon M. White^e, Thorfinnur Gunnlaugsson^{b*} and Frederick M. Pfeffer^{a*}

Graphical abstract



A humble norbornene functions as an ionic orgelator, forms aqueous biphasic and triphasic systems and assembles to form chiral helices.

